

# How warm is too warm? Towards robust Lyman- $\alpha$ forest bounds on warm dark matter

A. Garzilli\* and O. Ruchayskiy

Discovery Center, Niels Bohr Institute, Copenhagen University,  
Blegdamsvej 17, DK-2100 Copenhagen, Denmark

A. Magalich and A. Boyarsky

Lorentz Institute, Leiden University, Niels Bohrweg 2, Leiden, NL-2333 CA, The Netherlands

(Dated: December 21, 2024)

The Lyman- $\alpha$  forest is a powerful tool to constrain warm dark matter models (WDM). Its main observable – flux power spectrum – should exhibit a suppression at small scales in WDM models. This suppression, however, can be mimicked by a number of thermal effects related to the instantaneous temperature of the intergalactic medium (IGM), and to the history of reionization and of the IGM heating (“*pressure effects*”). Therefore, to put robust bounds on WDM one needs to disentangle the effect of free-streaming of dark matter particles from the influence of all astrophysical effects. This task cannot be brute-forced due to the complexity of the IGM modelling. In this work, we model the sample of high-resolution and high-redshift quasar spectra (Boera *et al.* 2019) assuming a thermal history that leads to the smallest pressure effects while still being broadly compatible with observations. We explicitly marginalize over observationally allowed values of IGM temperature and find that (thermal) WDM models with masses above 1.9 keV (at 95% CL) are consistent with the spatial shape of the observed flux power spectrum at  $z = 4 - 5$ . Even warmer models would produce a suppression at scales that are larger than observed, independently of assumptions about thermal effects. This bound is significantly lower than previously claimed bounds, demonstrating the importance of the knowledge about the reionization history and of the proper marginalization over unknowns.

**Warm dark matter.** Dark matter (DM) in the Universe manifests itself through many distinct observations – from rotational curves of stars in galaxies to the statistics of anisotropies of cosmic microwave background (CMB) [2]. If dark matter is made of particles – little is known about their properties. One such property, that can be learned from the cosmological data, is the *free-streaming horizon*,  $\lambda_{\text{DM}}$ , – the distance that particles travel while being relativistic (see *e.g.* [3] for the definition). Such particles are known as *warm dark matter* (WDM), as opposed to *cold dark matter* (CDM) particles that only streamed while being already non-relativistic. This quantity is of interest, because it is related to the production mechanism of DM particles in the early Universe. The scale  $\lambda_{\text{DM}}$  is a characteristic scale below which matter power spectrum of WDM models is suppressed as compared to the CDM with the same cosmological parameters, as relativistic particles smooth out primordial inhomogeneities.

Many particle physics candidates can play the role of warm dark matter (including sterile neutrinos [4], axinos [5, 6], gravitinos [7]). In this work by “WDM” we refer to a specific class where DM is produced in thermal equilibrium, and then freezes out – (*warm*) *thermal relics* or “thermal WDM” [8]. In this case there is a one-to-one relation between  $\lambda_{\text{DM}}$  and the DM particle mass,  $m_{\text{WDM}}$  ( $\lambda_{\text{DM}} \propto m_{\text{WDM}}^{-4/3}$ ), see *e.g.* [9]. Although “thermal WDM” does not correspond to any specific particle

physics model<sup>1</sup> parametrization is often chosen when deriving WDM constraints.

The formation of structures in WDM is suppressed for perturbations of comoving size  $\lesssim \lambda_{\text{DM}}$  [13]. However, once overdensities of scales  $\sim \lambda_{\text{DM}}$  reach critical threshold, the nonlinear process quickly brings WDM power spectrum close to its CDM counterpart at these scales. Therefore, the most discriminating power between CDM and WDM lies at small scales. One of the promising tools to measure this difference is the *Lyman- $\alpha$  forest method* [3, 14–22].

**Lyman- $\alpha$  forest.** Residual neutral hydrogen gas in the intergalactic medium (IGM) creates a “forest” of absorption features in the spectra of high-redshift background quasars. These absorption features are the results of the Lyman- $\alpha$  transition  $n = 1 \rightarrow 2$  (see *e.g.* [23] for review). The Fourier transform of the absorption lines’ auto-correlation function in the velocity space gives rise to the *flux power spectrum* (FPS)  $\Delta_F^2(k)$  – a proxy to the matter power spectrum projected to 1D along the line of sight, see *e.g.* [23]. The neutral gas follows the underlying dark matter relatively well, which allows to

---

<sup>1</sup> Thermal WDM particles would have decoupled much earlier than the ordinary neutrinos. As a result their number density would exceed that of cosmic neutrinos ( $n_{\text{WDM}} \gg 112 \text{ cm}^{-3}$ ). For fermionic DM, whose mass obeys the Tremaine-Gunn bound [10],  $m_{\text{WDM}} \gtrsim 300 \text{ eV}$  [11] this would mean a matter density too large, as compared to  $\rho_{\text{DM}}$  and significant entropy dilution needs to be arranged in order to reconcile the density of thermal WDM particles with observations, see *e.g.*, [12].

use the flux power spectrum as a proxy of matter power spectrum at small scales and, in particular, to probe free streaming properties of DM particles [3, 14–22, 24–26].

In this work we use the high resolution and high redshift data of [1]. The observed power spectrum  $\Delta_F^2$  exhibits a cut-off on scales below  $\lambda_F \approx 30 \text{ km s}^{-1}$  at  $z \sim 5$  [1]. The same cutoff is visible in the older dataset by HIRES [27] and MIKE [28], used in [18, 19, 22, 25, 26]. This does not mean, however, that warm dark matter with  $\lambda_{\text{DM}} \sim \lambda_F$  has been discovered! Indeed, several thermal effects may prevent HI from following DM at small scales [29, 30]:

(a) IGM is heated as a result of reionization and the thermal Doppler broadening of the absorption lines due to the Maxwellian velocities introduces its own cutoff in the flux power spectrum. The temperature of the gas, and hence the level of Doppler broadening,  $\lambda_b$ , that needs to be applied, is not accurately known (see *e.g.* [19, 31]), especially at redshifts  $z \gtrsim 5$  [32–35]. This effect is due to the IGM temperature at the time of observation.

(b) The absorbing filaments in the IGM are not virialized structures, and therefore their typical size depends on the past thermal history, relatively to the time of observation. The gas distribution is smoothed compared to the dark matter due to pressure [29, 36], with its own cutoff  $\lambda_p$ . Because of the absence of the Gunn-Peterson trough at redshift  $z < 6$ , we know that the IGM was reionized, presumably by photo-heating from ultraviolet producing sources [23]. Hydrogen reionization is thought to be completed by  $z = 5.7$  [37–39] and to start not earlier than  $z = 8$  [40], the details about this process are mostly unknown (see *e.g.* [41–43]).

**Our method.** Work [22] has demonstrated that the cutoff observed in the measured FPS can be explained by any of the three effects (Doppler, pressure, DM free-streaming). This means that in order to obtain *robust* constraints on the properties of WDM particles one would need to marginalize over all astrophysical effects that can produce similar suppression in the FPS. The marginalisation over thermal histories (=pressure effects) cannot be computed by brute-force: each thermal history requires its own full scale hydrodynamical simulation. On the other hand, marginalisation over Doppler broadening is possible in post-processing and is not computationally expensive.

Therefore, in this work we suggest the following procedure for obtaining *robust Lyman- $\alpha$  forest bounds*:

(1) In order to minimise the pressure effects, we run hydrodynamical simulations with model of ultraviolet background (UVB) LATECOLD from [41].<sup>2</sup> In this model the reionization starts at redshift  $z = 6.7$ , later than

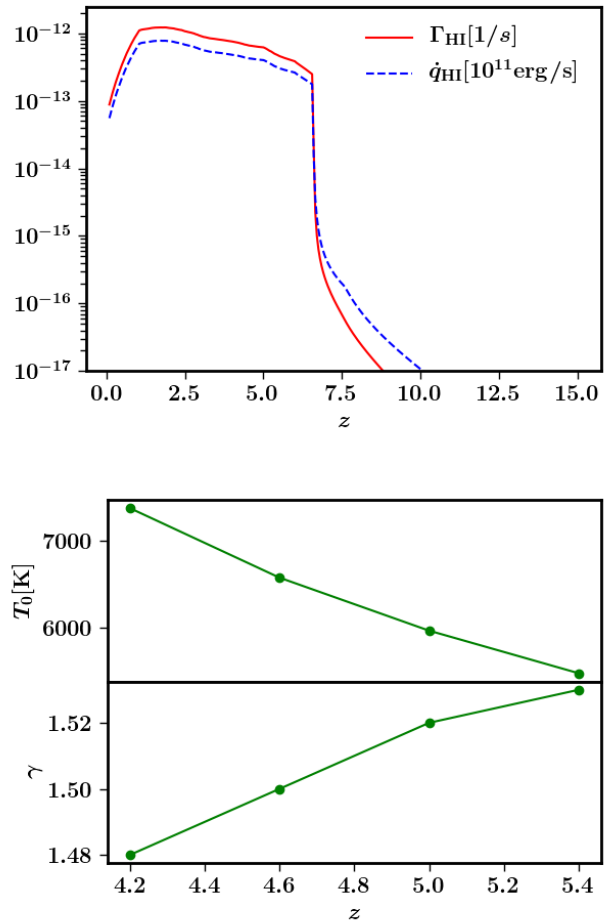


FIG. 1. The adopted thermal history. In the upper panel we show the photoionization ( $\Gamma_{\text{HI}}$ ) and photoheating ( $\dot{q}_{\text{HI}}$ ) rates for the neutral hydrogen (HI) from the LATECOLD model of Oñorbe *et al.* [41]. The photoheating rate is rescaled by  $10^{11}$  in order to fit onto the same plot. The reionization in this model starts at  $z_{\text{reio}} = 6.7$ . In the lower panel we show the resulting temperature at the cosmic mean density of the IGM,  $T_0$ , as well as the slope of the temperature-density relation,  $\gamma(z)$  (obtained by fitting the Eq. (1) to the simulation snapshots).

other thermal histories, considered in [41] or by other groups. Nevertheless, LATECOLD scenario reproduces the measured temperature at post-reionization redshift  $z \sim 5$  compatible with the constraint on reionization time [41]. By construction it gives the minimal filaments size.<sup>3</sup> We have assumed that the intergalactic medium is optically thin, and that reionization happens uniformly in all the space.

<sup>3</sup> We thank J. Oñorbe for sharing with us the data of the LATECOLD thermal history that were not published together with the other thermal histories in [41]. HI photo-heating and photoionization rates are shown in Fig. 1.

<sup>2</sup> The details about the numerical simulations can be found in [22].

Name	$L$ [Mpc/ $h$ ]	$N$	Dark matter	UVB
CDM	20	$1024^3$	CDM	LATECOLD
WDM	same	same	$m_{\text{WDM}} = 2 \text{ keV}$	same
EAGLE_REF	$100 h$	$1504^3$	CDM	EAGLE

TABLE I. Hydrodynamical simulations considered in this work together with corresponding parameters. All simulations were performed specifically for this work, except `EAGLE_REF` [44]. Columns contain from left to right: simulation identifier, co-moving linear extent of the simulated volume ( $L$ ), number of dark matter particles ( $N$ ; also equal to the number of gas particles), type of dark matter (CDM or WDM),  $m_{\text{WDM}}$  (expressed in natural units), ultra-violet background imposed during the simulation (LATECOLD refers to a reionization model in agreement with measured temperature of the IGM as discussed in Oñorbe *et al.* [41], see Fig. 1; EAGLE indicates the standard UVB from [45]). The cosmological parameters are chosen according to Table II. The gravitational softening length for gas and dark matter is kept constant in co-moving coordinates at  $1/30^{\text{th}}$  of the initial interparticle spacing. All simulations start from the initial conditions generated by the 2LPTic [46] with the same ‘glass’-like particle distribution generated by GADGET-2 [47].

Cosmology	<i>Planck</i> [48]
$\Omega_0$	$0.308 \pm 0.012$
$\Omega_\Lambda$	$0.692 \pm 0.012$
$\Omega_b h^2$	$0.02226 \pm 0.00023$
$h$	$0.6781 \pm 0.0092$
$n_s$	$0.9677 \pm 0.0060$
$\sigma_8$	$0.8149 \pm 0.0093$

TABLE II. Cosmological parameters used in our simulations. *Planck* cosmology is the conservative choice of TT+lowP+lensing from Ade *et al.* [48] (errors represent 68% confidence intervals).

(2) We explicitly marginalise over the IGM temperature (*Doppler broadening*) adding their effects to the FPS in post-processing. The IGM temperature depends on the matter density  $\Delta = \rho/\bar{\rho}_M$  and can be described by a power-law in the density of the IGM [49]:

$$T = T_0 \left( \frac{\rho}{\bar{\rho}} \right)^{\gamma-1} \quad (1)$$

where  $\rho$  is the matter density of a small patch of the Universe and  $\bar{\rho}$  is the background matter density. Because the Lyman  $\alpha$  forest at each redshift is sensitive only to a short range of densities, we model the IGM temperature with a single value,  $T_0$ . This is additionally justified by the fact that in the approximation of instantaneous reionization, that we are using, all the part of the IGM get to the same temperature at the same time, hence  $\gamma = 1.0$ , *i.e.*, there is no dependence of temperature on density.

(3) We also marginalise over the *effective optical depth*  $\tau_{\text{eff}} = -\ln\langle F \rangle$ , where  $F$  is the transmitted flux, and  $\langle \dots \rangle$  is the average.  $\tau_{\text{eff}}$  encompasses the information about the average absorption level (*i.e.* overall level of ionization of the IGM). The work [1] provided measurements of  $\tau_{\text{eff}}$  in each of the redshift bins together with the errorbars. We can vary  $\tau_{\text{eff}}$  in the post-processing of the spectra, by rescaling the optical depth in the spectra by a suitable factor.

**Data and Covariance matrix.** The HIRES sample of high resolution quasar spectra at  $z > 4$ , released by Boera *et al.* [1], consists of 14 Lyman  $\alpha$  forest spectra over the redshift range  $4.0 \leq z \leq 5.2$ . These spectra are binned into three redshift intervals of width  $\Delta z = 0.4$ , centered on  $z = 4.2, 4.6, 5.0$ . Their total comoving length per redshift interval is  $L = 1412, 2501, 1307 \text{ Mpc}/h$ . By construction the Lyman- $\alpha$  data points are strongly correlated [50]. The covariance matrices have been estimated in [1] from the data, using ‘bootstrap method’. While bootstrap method is widely used in the literature for estimating the covariance matrix, it can only evaluate covariance due to the scatter within the sample (see *e.g.*, [50]). From the data one cannot estimate, however, how representative the sample is – this contribution is also commonly called *sample variance*. Because of the smallness of the sample size the sample variance can be an important contribution to the covariance matrix. We try to estimate it using the simulations. To properly recover a covariance matrix from the simulations, one needs a simulation box whose size is comparable with the comoving length of the spectra (see *e.g.*, discussion in Garzilli *et al.* [22]). A typical length of a single Lyman- $\alpha$  forest spectrum is  $\sim 200 \text{ cMpc}$ , while our simulation box is  $20 \text{ cMpc}$ .

In order to evaluate the covariance matrix we took the EAGLE simulation with  $L = 100 \text{ Mpc}/h$  and  $N_{\text{part}} = 1504^3$  [44]. These simulations do not have the resolution needed for the smallest scales measured in the dataset (see the discussion in [22]). For this reason, we approximate the covariance matrix with the following procedure. We computed the expected covariance matrix from the above mentioned EAGLE simulation run by bootstrap, considering a mock data sample of the length equivalent to that of the observed data sample. For each redshift interval, we consider the snapshot at the central redshift. We extract 1000 mock spectra. We compute the FPS for each mock spectrum. We group the mock spectra in sub-samples with the same comoving length as the data-sample, and for each mock sub-sample we compute the average of the FPS. The covariance matrix is computed with the average FPS with respect to the average

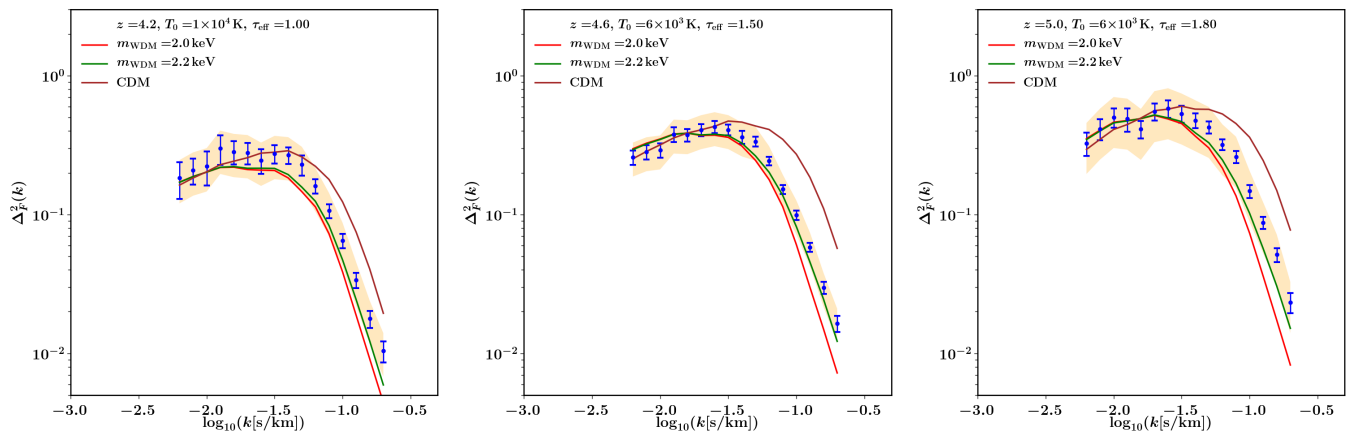


FIG. 2. Data of Boera *et al.* together with several cosmological models: WDM with  $m_{\text{WDM}} = 2 \text{ keV}$  (red line, compatible with the data at 95% CL), WDM with  $m_{\text{WDM}} = 2.2 \text{ keV}$  (green line) and CDM (brown line). The thermal history LATECOLD from [41] with late redshift of reionization  $z_{\text{reio}} = 6.7$  is used for all three models. Orange shaded region indicates the level of uncertainty of the data, related to the sample variance (estimated from the simulations, see text for details).

FPS computed on all the mock spectra. After that, we compute the maximum relative errors obtained by comparing the diagonal elements of the covariance matrix to the data. Hence, we rescale all elements of the covariance matrix to this same maximum relative error. Our normalized matrices are comparable with those of [1], the difference can be attributed to a different resolution. Indeed, we checked that insufficient resolution *increases* a correlation between data points.

**Data analysis.** Our resulting model describing evolution of FPS contains 7 parameters: inverse WDM mass  $[\text{keV}]/m_{\text{WDM}}$ , IGM temperature at the cosmic mean density and  $\tau_{\text{eff}}$  (the latter two quantities are evaluated at redshifts  $z = 4.2, 4.6, 5.0$ ). We consider linear priors on the temperature and logarithmic priors on the mass of warm dark matter. In order to get theoretical predictions of the FPS, we run our simulations for two distinct cosmological models: CDM, and thermal relic WDM with mass 2 keV. Starting from our simulations, we compute in post-processing the FPS for the parameter arranged on a three-dimensional regular grid in  $k$ -space. Our final theoretical model is obtained by interpolating linearly the FPS across the grid. We perform a joint analysis on all the redshift intervals.

**Results.** We explore the likelihood via the Monte Carlo Markov Chains (MCMC). The  $1\sigma$  and  $2\sigma$  contours of the cosmic mean temperature,  $T_0$ , the optical depth,  $\tau$ , and the mass of the WDM,  $m_{\text{WDM}}$  are shown in Figure 3. By marginalizing over  $T_0(z)$  and  $\tau(z)$  we find the lower limit on the warm dark matter  $m_{\text{WDM}} \geq 1.9 \text{ keV}$  at 95% CL. Warmer WDM models are excluded regardless of the instantaneous temperature of IGM, as the contours in Fig. 3 demonstrate. For each mass we also find the *upper bound* on  $T_0(z)$  at redshifts  $z = 4.2, 4.6, 5.0$ , see

Fig. 4. A complete set of 2D plots are shown in Fig. 5. We have repeated the MCMC exploration using the covariance matrix provided by [1], albeit with the errorbars inflated to account for the sample variance. The resulting contours changed only slightly with the 95% CL for the mass reaching 2.05 keV.

As our procedure is somewhat different from a standard MCMC exploration of the likelihood, we have several comments:

1. Our contours do not reach the CDM values ( $1/m_{\text{WDM}} = 0$ ). This does not mean that the CDM cosmology is excluded by the data. This indicates that in the LATECOLD reionization scenario with cold DM, the temperature alone would not be sufficient to explain the suppression of the FPS. Therefore, in CDM cosmology the LATECOLD model would be ruled out, while in the WDM cosmology with  $m_{\text{WDM}} > 1.9 \text{ keV}$  it is actually allowed. Ref. [51] studied the dataset of [18] and found that cold DM model with LATECOLD reionization is consistent with the data, but they did not study the dataset [1] we have considered in this work.
2. For the same reason our upper limits on the temperature (Fig. 4) are, probably, exaggerated as they compensate minimal pressure history. While for the LATECOLD history these are 95% CL upper bounds, for other thermal histories at similar confidence level one would be getting lower temperatures. Thus, one can treat them as (overly) conservative upper bounds on  $T_0$ . We do not provide lower bounds on the temperature as they are not meaningful.

**Conclusion and future work.** We have produced new

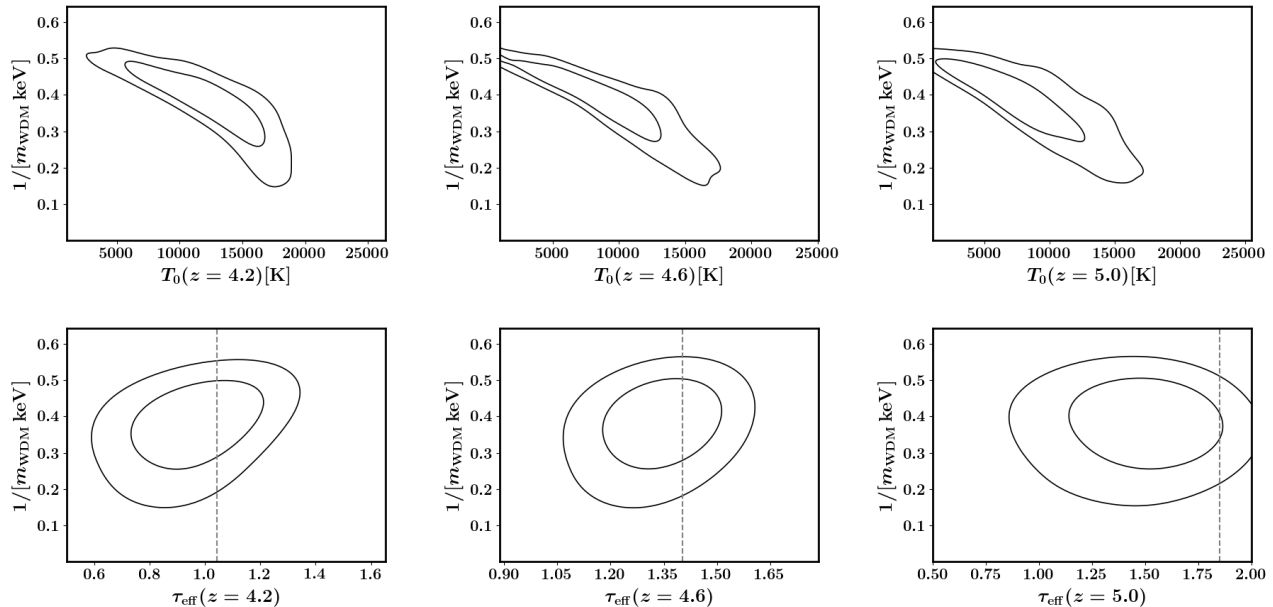


FIG. 3. Confidence regions between the WDM mass,  $m_{\text{WDM}}$ , the IGM mean temperature,  $T_0$  and the effective optical depth  $\tau_{\text{eff}}$  at redshifts  $z = 4.2, 4.6, 5.0$ . Our analysis shows that if LATECOLD were a true history of reionization, then the CDM would be ruled out. However, it is not possible to use this analysis to determine the IGM temperature in CDM for reionization histories outside LATECOLD. For the same reason our analysis does not allow to determine robust *lower* bounds on  $T_0$  for a given WDM mass. The (conservative) upper bounds are shown in Fig. 4.

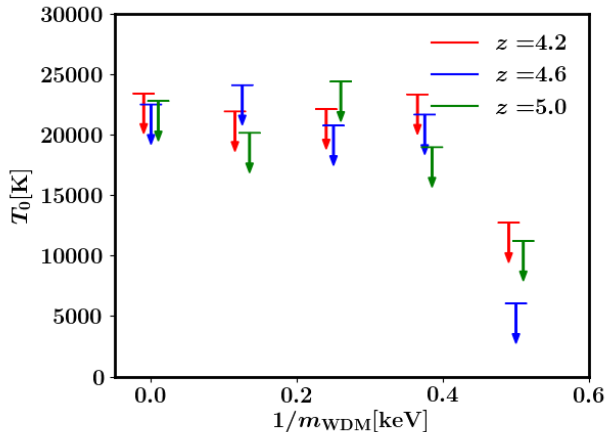


FIG. 4. The  $2\text{-}\sigma$  level upper limit on  $T_0$  as a function of  $1/m_{\text{WDM}}$ . The upper limit has been estimated separately for each redshift interval with fixed  $m_{\text{WDM}}$ . We only show the mass interval between  $m_{\text{WDM}} = 2\text{ keV}$  and CDM. This result is in substantial agreement with the global fit that we have shown in Figure 3. These bounds are fully consistent with existing estimates of the IGM temperatures at redshifts  $z = 4 - 5$  [see *e.g.*, 32, 33, 52, 53]. One should keep in mind that these works evaluated IGM temperatures for CDM cosmology only and for some limited class of thermal histories, not necessarily consistent with LATECOLD.

using the high resolution Lyman- $\alpha$  forest dataset of [1]. When deriving bounds on DM properties it is important to marginalize over all possible astrophysical uncertainties in a conservative way. Marginalization over thermal histories is not a straightforward procedure. In order to do so, we have used a highly conservative thermal history for the IGM that gives a minimal size of the intergalactic structures. This thermal history minimizes the pressure effects. We have also explicitly marginalized over the Doppler broadening, finding that WDM thermal relics with mass as low as 1.9 keV are consistent with the data at 95% CL. Our procedure lowers the Lyman- $\alpha$  bound significantly compared to  $m_{\text{WDM}} \geq 3.3\text{ keV}$  obtained from the HIRES/MIKE data by [18] (for detailed comparison between assumed thermal histories in these works see the discussion in [19, 22]).<sup>4</sup> In terms of the characteristic free-streaming length,  $\lambda_{\text{DM}}$  our bound is two times weaker. Thus, although the difference between CDM and WDM is the most pronounced at small scales, the influence of astrophysical effects is also the largest there. Therefore, it becomes interesting to compare our results with those, obtained from the lower resolution SDSS Lyman- $\alpha$  data datasets. These data have several advantages that may help to reduce this systematic uncertainty: reduced sample variance due to the

constraint on the mass of warm dark matter particles

<sup>4</sup> All limits quoted at this section are at 95% CL.

large number of quasars; less pronounced dependence on astrophysical processes on larger scales. Using the SDSS dataset [17] found  $m_{\text{WDM}} \gtrsim 2.5$  keV (see also [16]) which ref. [3] reduced to  $m_{\text{WDM}} \geq 1.7$  keV, using a more conservative treatment of the systematic uncertainties. The most recent analysis based on the SDSS-III/BOSS dataset [20, 21] found  $m_{\text{WDM}} \geq 3.06$  keV (when using Planck cosmological parameters). These works did not explore the influence of the thermal histories similar to LATECOLD used here, implicitly assuming that such a relevance is greatly reduced at larger scales and smaller redshifts that BOSS dataset probes. We leave investigation of this question for a future work.

In this work we adopted LATECOLD reionization history as the one, providing minimal pressure support, consistent with existing data. Whether this is the case in non-CDM cosmologies (not explored in [41]) or whether minimal Jeans scale  $\lambda_J$  can be estimated by other methods (*e.g.*, [19, 54]) or from other data (see *e.g.*, [55]) remains to be seen.

**Note added.** When this work was complete, a paper [56] appeared that claims a several times stronger bound from eBOSS Lyman- $\alpha$  forest dataset [57]. At scales probed by this dataset ( $k < 0.02$  sec/km which translates at  $k \sim 2$  h/Mpc at redshifts  $z \sim 4$ ) the distinction between CDM and WDM with  $m_{\text{WDM}} \sim 10$  keV is small. To claim such a precision of determination of power spectrum, one needs to control all possible systematics at a comparable level. In particular, the uncertainty due to different thermal histories and therefore, different pressure effects at scales, probed by eBOSS (however small) need to be marginalized over. Therefore, to fully use the high-statistics eBOSS dataset, a lot of progress on theoretical side should be made and, in particular, realistic high-resolution simulations, assuming different alternative UV backgrounds and different thermal histories should be performed. This analysis will be performed elsewhere.

**Acknowledgments.** This project has received funding from the European Research Council (ERC) under the European Union’s Horizon 2020 research and innovation programme (ERC Advanced Grant 694896). This work used the DiRAC Data Centric system at Durham University, operated by the Institute for Computational Cosmology on behalf of the STFC DiRAC HPC Facility ([www.dirac.ac.uk](http://www.dirac.ac.uk)). This equipment was funded by BIS National E-infrastructure capital grant ST/K00042X/1, STFC capital grants ST/H008519/1 and ST/K00087X/1, STFC DiRAC Operations grant ST/K003267/1 and Durham University. DiRAC is part of the National E-Infrastructure. AM is supported by the Netherlands Organization for Scientific Research (NWO) under the program ”Observing the Big Bang” of the Organization for Fundamental Research in Master (FOM).

We would like to thank Jose Oñorbe for sharing with us additional unpublished thermal histories.

---

\* [garzilli@nbi.ku.dk](mailto:garzilli@nbi.ku.dk)

- [1] E. Boera, G. D. Becker, J. S. Bolton, and F. Nasir, *Astrophys. J.* **872**, 101 (2019), [arXiv:1809.06980](https://arxiv.org/abs/1809.06980) [[astro-ph.CO](https://arxiv.org/archive/astro)].
- [2] P. J. E. Peebles, *Nat. Astron.* **1**, 0057 (2017), [arXiv:1701.05837](https://arxiv.org/abs/1701.05837) [[astro-ph.CO](https://arxiv.org/archive/astro)].
- [3] A. Boyarsky, J. Lesgourgues, O. Ruchayskiy, and M. Viel, *J. Cosmology Astropart. Phys.* **5**, 012 (2009), [arXiv:0812.0010](https://arxiv.org/abs/0812.0010).
- [4] A. Boyarsky, M. Drewes, T. Lasserre, S. Mertens, and O. Ruchayskiy, *Prog. Part. Nucl. Phys.* **104**, 1 (2019), [arXiv:1807.07938](https://arxiv.org/abs/1807.07938) [[hep-ph](https://arxiv.org/archive/hep)].
- [5] L. Covi, H.-B. Kim, J. E. Kim, and L. Roszkowski, *JHEP* **05**, 033 (2001), [arXiv:hep-ph/0101009](https://arxiv.org/abs/hep-ph/0101009) [[hep-ph](https://arxiv.org/archive/hep)].
- [6] K.-Y. Choi, J. E. Kim, and L. Roszkowski, *J. Korean Phys. Soc.* **63**, 1685 (2013), [arXiv:1307.3330](https://arxiv.org/abs/1307.3330) [[astro-ph.CO](https://arxiv.org/archive/astro)].
- [7] T. Moroi, H. Murayama, and M. Yamaguchi, *Phys. Lett.* **B303**, 289 (1993).
- [8] P. Bode, J. P. Ostriker, and N. Turok, *Astrophys. J.* **556**, 93 (2001), [arXiv:astro-ph/0010389](https://arxiv.org/abs/astro-ph/0010389) [[astro-ph](https://arxiv.org/archive/astro)].
- [9] A. Boyarsky, J. Lesgourgues, O. Ruchayskiy, and M. Viel, *Phys. Rev. Lett.* **102**, 201304 (2009), [arXiv:0812.3256](https://arxiv.org/abs/0812.3256) [[hep-ph](https://arxiv.org/archive/hep)].
- [10] S. Tremaine and J. E. Gunn, *Physical Review Letters* **42**, 407 (1979).
- [11] A. Boyarsky, O. Ruchayskiy, and D. Iakubovskiy, *J. Cosmology Astropart. Phys.* **0903**, 005 (2009), [arXiv:0808.3902](https://arxiv.org/abs/0808.3902) [[hep-ph](https://arxiv.org/archive/hep)].
- [12] F. Bezrukov, H. Hettmansperger, and M. Lindner, *Phys. Rev.* **D81**, 085032 (2010), [arXiv:0912.4415](https://arxiv.org/abs/0912.4415) [[hep-ph](https://arxiv.org/archive/hep)].
- [13] R. Adhikari *et al.*, *J. Cosmology Astropart. Phys.* **1701**, 025 (2017), [arXiv:1602.04816](https://arxiv.org/abs/1602.04816) [[hep-ph](https://arxiv.org/archive/hep)].
- [14] S. H. Hansen, J. Lesgourgues, S. Pastor, and J. Silk, *Mon. Not. Roy. Astron. Soc.* **333**, 544 (2002), [arXiv:astro-ph/0106108](https://arxiv.org/abs/astro-ph/0106108) [[astro-ph](https://arxiv.org/archive/astro)].
- [15] M. Viel, J. Lesgourgues, M. G. Haehnelt, S. Matarrese, and A. Riotto, *Phys. Rev.* **D71**, 063534 (2005), [arXiv:astro-ph/0501562](https://arxiv.org/abs/astro-ph/0501562) [[astro-ph](https://arxiv.org/archive/astro)].
- [16] M. Viel, J. Lesgourgues, M. G. Haehnelt, S. Matarrese, and A. Riotto, *Phys. Rev. Lett.* **97**, 071301 (2006), [arXiv:astro-ph/0605706](https://arxiv.org/abs/astro-ph/0605706) [[astro-ph](https://arxiv.org/archive/astro)].
- [17] U. Seljak, A. Makarov, P. McDonald, and H. Trac, *Phys. Rev. Lett.* **97**, 191303 (2006), [arXiv:astro-ph/0602430](https://arxiv.org/abs/astro-ph/0602430) [[astro-ph](https://arxiv.org/archive/astro)].
- [18] M. Viel, G. D. Becker, J. S. Bolton, and M. G. Haehnelt, *Phys. Rev. D* **88**, 043502 (2013), [arXiv:1306.2314](https://arxiv.org/abs/1306.2314) [[astro-ph.CO](https://arxiv.org/archive/astro)].
- [19] A. Garzilli, T. Theuns, and J. Schaye, *Mon. Not. Roy. Astron. Soc.* **450**, 1465 (2015), [arXiv:1502.05715](https://arxiv.org/abs/1502.05715) [[astro-ph.CO](https://arxiv.org/archive/astro)].
- [20] J. Baur, N. Palanque-Delabrouille, C. Yèche, C. Magneville, and M. Viel, *J. Cosmology Astropart. Phys.* **8**, 012 (2016), [arXiv:1512.01981](https://arxiv.org/abs/1512.01981).
- [21] J. Baur, N. Palanque-Delabrouille, C. Yèche, A. Boyarsky, O. Ruchayskiy, É. Armengaud, and J. Lesgourgues, *J. Cosmology Astropart. Phys.* **12**, 013 (2017),

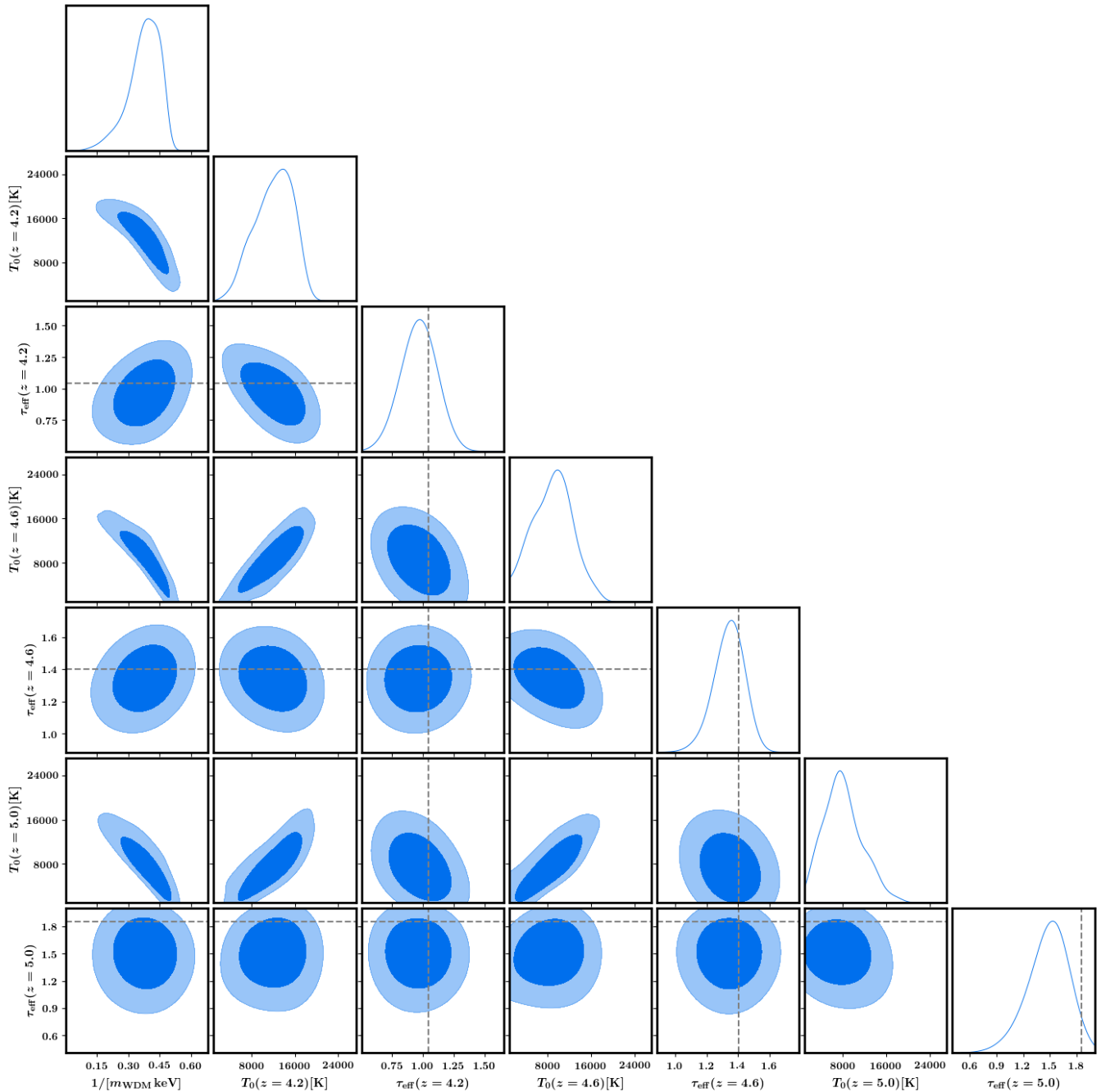


FIG. 5. Confidence regions between the WDM mass,  $m_{\text{WDM}}$ , the IGM mean temperature,  $T_0$  and the effective optical depth,  $\tau_{\text{eff}}$ , at redshifts  $z = 4.2, 4.6, 5.0$ . The dashed grey lines are the  $\tau_{\text{eff}}$  as measured in [1].

- arXiv:1706.03118.
- [22] A. Garzilli, A. Magalich, T. Theuns, C. S. Frenk, C. Weniger, O. Ruchayskiy, and A. Boyarsky, *Mon. Not. Roy. Astron. Soc.*, 2103 (2019), arXiv:1809.06585 [astro-ph.CO].
- [23] A. A. Meiksin, *Reviews of Modern Physics* **81**, 1405 (2009), arXiv:0711.3358.
- [24] M. Viel, G. D. Becker, J. S. Bolton, M. G. Haehnelt, M. Rauch, and W. L. W. Sargent, *Phys. Rev. Lett.* **100**, 041304 (2008), arXiv:0709.0131 [astro-ph].
- [25] V. Iršič, M. Viel, M. G. Haehnelt, J. S. Bolton, S. Cristiani, G. D. Becker, V. D’Odorico, G. Cupani, T.-S. Kim, T. A. M. Berg, S. López, S. Ellison, L. Christensen, K. D. Denney, and G. Worseck, *Phys. Rev. D* **96**, 023522 (2017), arXiv:1702.01764.
- [26] R. Murgia, V. Iršič, and M. Viel, ArXiv preprint (2018), arXiv:1806.08371 [astro-ph.CO].
- [27] S. S. Vogt *et al.*, *Proc. SPIE Int. Soc. Opt. Eng.* **2198**, 362 (1994).
- [28] G. M. Bernstein, A. E. Athey, R. Bernstein, S. M. Gun-

- nels, D. O. Richstone, and S. A. Shectman, “Volume-phase holographic spectrograph for the Magellan telescopes,” in *Proc. SPIE Vol. 4485, p. 453-459, Optical Spectroscopic Techniques, Remote Sensing, and Instrumentation for Atmospheric and Space Research IV, Allen M. Larar; Martin G. Mlynczak; Eds.*, Society of Photo-Optical Instrumentation Engineers (SPIE) Conference Series, Vol. 4485, edited by A. M. Larar and M. G. Mlynczak (2002) pp. 453–459.
- [29] N. Y. Gnedin and L. Hui, *Mon. Not. Roy. Astron. Soc.* **296**, 44 (1998), [astro-ph/9706219](#).
- [30] M. S. Peeples, D. H. Weinberg, R. Davé, M. A. Fardal, and N. Katz, *Mon. Not. Roy. Astron. Soc.* **404**, 1281 (2010), [arXiv:0910.0256 \[astro-ph.CO\]](#).
- [31] A. Rorai, R. F. Carswell, M. G. Haehnelt, G. D. Becker, J. S. Bolton, and M. T. Murphy, *Mon. Not. Roy. Astron. Soc.* **474**, 2871 (2018), [arXiv:1711.00930](#).
- [32] J. S. Bolton, G. D. Becker, S. Raskutti, J. S. B. Wyithe, M. G. Haehnelt, and W. L. W. Sargent, *Mon. Not. Roy. Astron. Soc.* **419**, 2880 (2012).
- [33] G. D. Becker, J. S. Bolton, M. G. Haehnelt, and W. L. W. Sargent, *Mon. Not. Roy. Astron. Soc.* **410**, 1096 (2011), [arXiv:1008.2622 \[astro-ph.CO\]](#).
- [34] J. S. Bolton, G. D. Becker, J. S. B. Wyithe, M. G. Haehnelt, and W. L. W. Sargent, *Mon. Not. Roy. Astron. Soc.* **406**, 612 (2010), [arXiv:1001.3415 \[astro-ph.CO\]](#).
- [35] L. Hui and Z. Haiman, *Astrophys. J.* **596**, 9 (2003).
- [36] T. Theuns, J. Schaye, and M. G. Haehnelt, *Mon. Not. Roy. Astron. Soc.* **315**, 600 (2000), [astro-ph/9908288](#).
- [37] G. D. Becker, J. S. Bolton, P. Madau, M. Pettini, E. V. Ryan-Weber, and B. P. Venemans, *Mon. Not. Roy. Astron. Soc.* **447**, 3402 (2015), [arXiv:1407.4850 \[astro-ph.CO\]](#).
- [38] J. Schroeder, A. Mesinger, and Z. Haiman, *Mon. Not. Roy. Astron. Soc.* **428**, 3058 (2013), [arXiv:1204.2838](#).
- [39] R. H. Becker *et al.* (SDSS), *Astron. J.* **122**, 2850 (2001), [arXiv:astro-ph/0108097 \[astro-ph\]](#).
- [40] R. Adam *et al.* (Planck), *Astron. Astrophys.* **596**, A108 (2016), [arXiv:1605.03507](#).
- [41] J. Oñorbe, J. F. Hennawi, and Z. Lukić, *Astrophys. J.* **837**, 106 (2017), [arXiv:1607.04218](#).
- [42] J. Oñorbe, J. F. Hennawi, Z. Lukić, and M. Walther, *Astrophys. J.* **847**, 63 (2017), [arXiv:1703.08633](#).
- [43] D. K. Hazra and G. F. Smoot, *J. Cosmology Astropart. Phys.* **1711**, 028 (2017), [arXiv:1708.04913 \[astro-ph.CO\]](#).
- [44] J. Schaye, R. A. Crain, R. G. Bower, and al., *Mon. Not. Roy. Astron. Soc.* **446**, 521 (2015), [arXiv:1407.7040](#).
- [45] F. Haardt and P. Madau, in *Clusters of Galaxies and the High Redshift Universe Observed in X-rays*, edited by D. M. Neumann and J. T. V. Tran (ArXiv [astro-ph/0106018](#), 2001) [arXiv:astro-ph/0106018](#).
- [46] R. Scoccimarro, L. Hui, M. Manera, and K. C. Chan, *Phys. Rev. D* **85**, 083002 (2012), [arXiv:1108.5512 \[astro-ph.CO\]](#).
- [47] V. Springel, *Mon. Not. Roy. Astron. Soc.* **364**, 1105 (2005), [astro-ph/0505010](#).
- [48] P. A. R. Ade *et al.* (Planck), *Astron. Astrophys.* **594**, A13 (2016), [arXiv:1502.01589 \[astro-ph.CO\]](#).
- [49] L. Hui and R. E. Rutledge, *Astrophys. J.* **517**, 541 (1999), [arXiv:astro-ph/9709100](#).
- [50] E. Rollinde, T. Theuns, J. Schaye, I. Pâris, and P. Petitjean, *Mon. Not. Roy. Astron. Soc.* **428**, 540 (2013).
- [51] M. Walther, J. Oñorbe, J. F. Hennawi, and Z. Lukić, *Astrophys. J.* **872**, 13 (2019), [arXiv:1808.04367 \[astro-ph.CO\]](#).
- [52] J. Schaye, T. Theuns, M. Rauch, G. Efstathiou, and W. L. W. Sargent, *Mon. Not. Roy. Astron. Soc.* **318**, 817 (2000), [astro-ph/9912432](#).
- [53] G. D. Becker, M. Rauch, and W. L. W. Sargent, *Astrophys. J.* **662**, 72 (2007), [arXiv:astro-ph/0607633 \[astro-ph\]](#).
- [54] A. Garzilli, T. Theuns, and J. Schaye, ArXiv e-prints (2018), [arXiv:1808.06646 \[astro-ph.CO\]](#).
- [55] K. N. Telikova, S. A. Balashev, and P. S. Shternin (2019) [arXiv:1911.03413 \[astro-ph.CO\]](#).
- [56] N. Palanque-Delabrouille, C. Yèche, N. Schöneberg, J. Lesgourgues, M. Walther, S. Chabanier, and E. Armengaud, (2019), [arXiv:1911.09073 \[astro-ph.CO\]](#).
- [57] S. Chabanier *et al.*, *J. Cosmology Astropart. Phys.* **1907**, 017 (2019), [arXiv:1812.03554 \[astro-ph.CO\]](#).